



Chapter 5:

Studies of Copper Schiff-base Complexes

Encapsulated in Zeolite Y and their Catalytic

Activity for the Styrene Oxidation Reaction

5.1. INTRODUCTION

Transformation of hydrocarbons into their oxyfunctionalized derivatives are the important chemical processes for the industrial and academic purpose. The synthesis of the carbonyl compounds, alcohols from olefins require the selective oxidation of the strong C-H bonds and it has been a challenge for long time.¹ Transition metal complexes are usually efficient catalysts for the oxidation of various organic compounds in mild reaction conditions; however these homogeneous catalysts always have some drawbacks e.g. instability, difficulty in the separation, lack of reusability and also the production of environmentally harmful chemicals as side products.²⁻⁴ The state-of-the-art of the catalytic science prefers such type of catalysts, which can overcome the limitations of the homogeneous catalytic processes without loss of reactivity. In this direction, heterogenisation of homogeneous catalyst is a convenient approach to couple the reactivity of the complex with the stability, specific environment provided by host materials and ease of separation. Impregnation and encapsulation of transition metal complexes in the microporous,⁵⁻⁸ mesoporous materials^{9, 10} and MOFs,^{11, 12} tagging homogeneous catalyst with ionic liquids,^{13, 14} and phase transfer catalyst^{15, 16} are some interesting examples of heterogeneous systems, which have been successfully employed in the various oxidation reactions by using H₂O₂, TBHP and molecular O₂ as oxidant.⁵ Zeolites, the microporous aluminosilicate materials are the competent hosts for the encapsulation of transition metal complexes with comparable molecular dimension with that of cavities of the host zeolites.^{7, 17} These contemporary classes of catalysts can afford a unique way to encapsulate the single-site catalyst molecule within the well structured architecture of the host, having large surface area. These systems have shown structural and functional analogy with cytochrome 450,¹⁸ and well explored as the proficient catalysts for the selective oxidative transformation of olefinic C-H bonds to its oxy-derivatives. P. Ratanasmy *et. al* have reported that both copper salen and 5-chloro copper salen complexes, when encapsulated in zeolite Y suffer from structural distortion and also are recognized as efficient catalysts for the oxidation of p-xylene and phenol. The authors also emphasize upon the fact that the presence of electron withdrawing group on the phenyl rings immensely improves the TOF, h⁻¹ of the oxidation reaction.³

Few more reports are available in literature, which also primarily identify the reason of enhanced reactivity as the distortion in the geometry of the guest complexes, under space

constraint imposed by zeolite framework. Maurya M. R *et. al* have studied catalytic activities of different metals complexes encapsulated in zeolite Y on the oxidation of different hydrocarbons such as styrene, cyclohexane, cyclohexene and methyl phenyl sulfide, where authors have evidently shown that encapsulated complexes are much more reactive for oxidative transformation than the corresponding free state complex.^{5, 19-23} Some other reports on the encapsulated metal phthalocyanine and tris(2,2' bipyridine) iron complexes for the oxidation reaction for phenols, styrene and methyl styrene also confirm that the free state complex especially tris(2,2' bipyridine) iron complex is definitely not so efficient catalyst like its encapsulated analogue in identical reaction conditions.^{24, 25} In another comparative study of different metal picolinato complexes in zeolite Y. R.C. Deka *et. al.* have observed that the copper and cobalt complexes are more reactive catalysts compared to the corresponding its nickel complexes for the selective oxidation of phenol by using H₂O₂ as oxidant.⁸ It is quite clear that the encapsulated complexes in zeolite Y are competent catalysts for oxidation transformation of hydrocarbons, and most of studies have suggested that enhanced activity of the encapsulated complex is definitely a consequence of the distorted geometry of the complex under space constraint inside the rigid cavity. In the present study, we have chosen the copper complexes with different substitution (-H, -OH, -Br and -OCH₃ on the 5th position of the phenyl rings) on the phenyl rings of Schiff base complexes, named as salen complexes are CuL1, CuL3, CuL4 and CuL6 on the basis of their increasing order of the molecular dimensions and encapsulated inside nearly spherical supercage of zeolite Y via flexible ligand synthesis method (given in Figure 5.1).

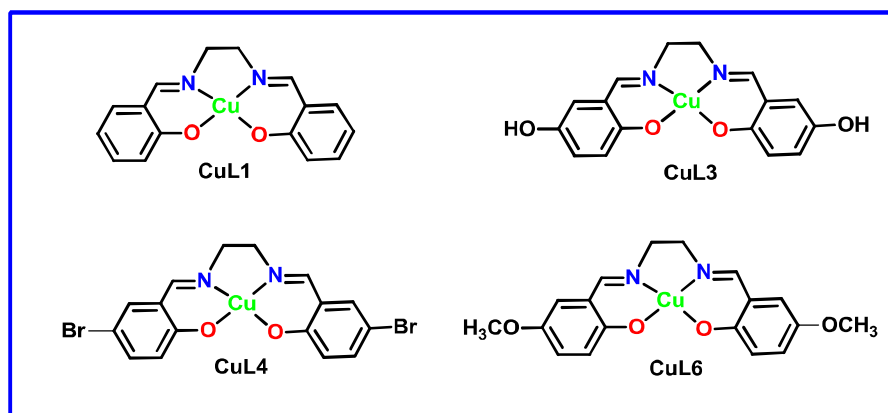


Figure 5.1: Schematic representation of copper Schiff base complexes.

These systems are well characterized with the help of powdered XRD, AAS, SEM-EDS, IR and UV-Visible spectroscopy. We have employed the systems as catalysts on the styrene oxidation reaction. Our major interest is to investigate whether such encapsulated complexes are more efficient as catalysts as compared to their neat form and if so, is there any correlation between the structure they adopt under encapsulation and catalytic activity of the guest complex; it is really interesting to know the diverse effects of molecular association e.g., steric and electronic effects and ligand architecture on the reactivity of the catalyst in homogeneous and heterogeneous state.

5.2. RESULTS AND DISCUSSION

Synthesis of ligands and copper Schiff-base complexes in free as well as in encapsulated states have already been discussed in chapter 2 under experimental section (2.2.1-2.2.6).

5.2.1. Elemental Analysis

Parent zeolite has Si/Al ratio is 2.34 whereas unit cell formula of host material is $\text{Na}_{58}\text{Al}_{58}\text{Si}_{136}\text{O}_{388} \cdot y\text{H}_2\text{O}$. The Si/Al ratio of host framework remains unaffected even after the complete synthesis of the metal complex inside it which no doubtably indicates the lack of dealumination during the whole process of ion exchange and encapsulation. The concentration of metals in different samples are determined by atomic absorption spectroscopy and it is found that the metal content in the encapsulated Cu complexes are always less than the metal content which is present in the Cu-exchanged zeolite Y (AAS data are given in Table 5.1). It has shown the possibility of the complex formation inside the host cavity or might be leaching of some metal ions during encapsulation process.

Table 5.1 AAS data of encapsulated complexes.

S.No	Samples	% weight of Cu
1	Cu-Y	0.81
2	CuL1-Y	0.62
3	CuL3-Y	0.59
4	CuL4-Y	0.37
5	CuL6-Y	0.39

5.2.2. X-Ray Diffraction and Scanning Electron Microscopy Analysis

To investigate the order of retention of zeolite crystallinity, surface morphology and integrity of host zeolite Y, XRD patterns of parent zeolite Y, Cu-zeolite Y and zeolite with encapsulated copper Schiff-base complexes are recorded (XRD patterns are given in Figure 5.2). Essentially similar patterns of all the samples indicate the preservation of integrity of host framework during the process of encapsulation. On comparison of the XRD patterns of encapsulated complexes with the pure and copper exchanged zeolite-Y, an evident distinction in the XRD patterns of the encapsulated complexes has been observed. Relative intensities of peaks at the $2\theta = 10^\circ$ and 12° , are altered after encapsulation. For parent zeolite and Cu-exchanged zeolite the relation $I_{220} > I_{311}$ exist, but for zeolite with encapsulated complexes the relation is just reverse; $I_{311} > I_{220}$. The observed alteration in these intensities after the encapsulation, has been empirically associated with the fact that a large complex is indeed present within the zeolite-Y supercage.²⁶

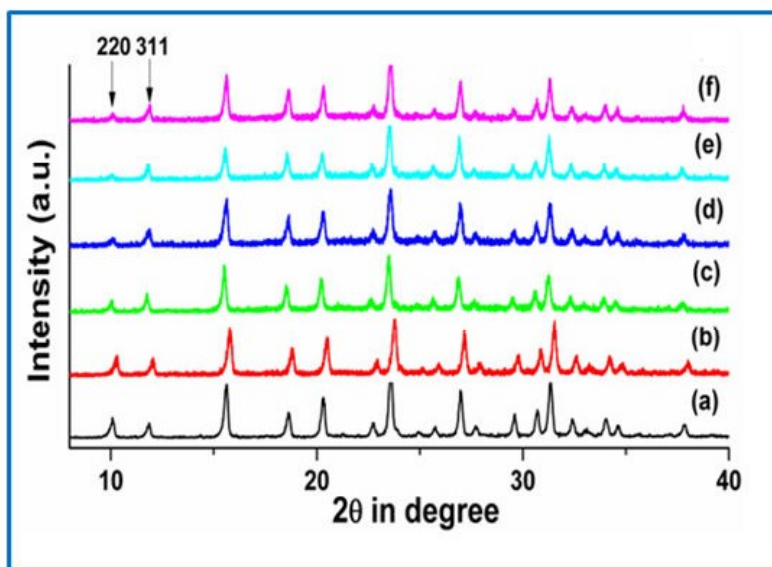


Figure 5.2: Powder XRD patterns of (a) pure zeolite-Y (b) Cu- exchanged zeolite-Y, (c) CuL1-Y, (d) CuL3-Y, (e) CuL4-Y and (f) CuL6-Y.

Scanning electron microscopy also supports the fact that the complex formation is primarily taking place inside the host cavities. From the SEM images (SEM micrographs given in Figure 5.3A is the encapsulated system before Soxhlet extraction and Figure 5.3 B-C are those after Soxhlet extraction).

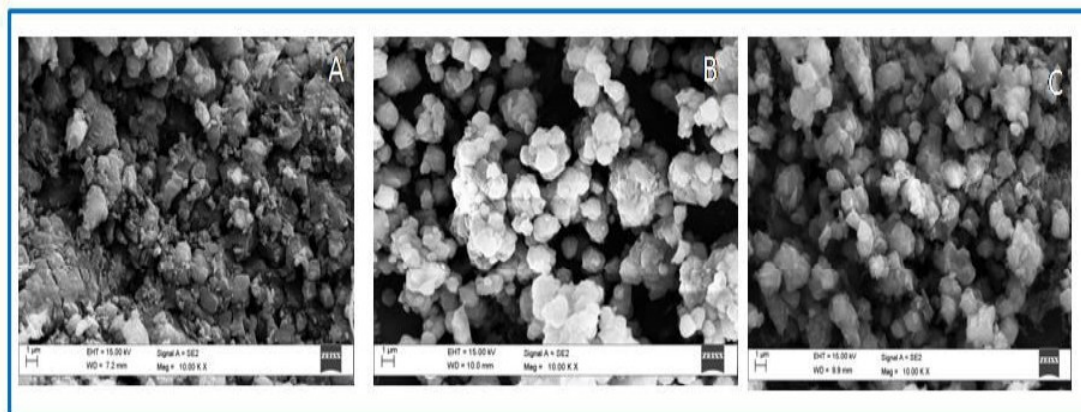


Figure 5.3: SEM images (A) CuL4-Y, before Soxhlet extraction and (B) CuL1-Y, (C) CuL4-Y after Soxhlet extraction.

It is observed that before Soxhlet extraction, there are some detectable surface species probably due to the formation of the complex at the surface or un-reacted ligands can be seen but these impurities are mostly vanished after Soxhlet extraction.²⁷ The clear noticeable boundaries of host lattice in SEM micrographs and change in the colour of Soxhlet extracted final product is certainly an indication of successful encapsulation of the complex inside the cavities of zeolite Y.

5.2.3. IR Spectroscopic study

IR spectra of ligands, (Figure 5.4) pure zeolite Y and all copper Schiff-base complexes in free and encapsulated states are given in Figure 5.4 and Table 5.2. Pure zeolite Y has shown strong IR peak at 1018 cm^{-1} , which is mainly attributed to the presence of asymmetric stretching vibrations of $(\text{Si}/\text{Al})\text{O}_4$ units of framework. Other some prominent peaks are present at 560 , 717 , 786 , 1643 and 3500 cm^{-1} position, which are mainly assigned to $(\text{Si}/\text{Al})\text{O}_4$ bending mode, double ring, symmetric stretching vibrations, other two IR bands at 1643 and 3500 cm^{-1} position are attributed to lattice water molecules and surface hydroxylic group respectively.^{8, 27} These IR bands are remaining unaffected even after encapsulation processes. All the encapsulated complexes have exhibited the bands without any significant alternation in the peak positions, evidently revealing the fact that host framework doesn't get modified during the complex formation inside the supercage. As discussed earlier, the suitable IR region for the characterization of encapsulated Schiff-base complex is $1200\text{-}1600\text{ cm}^{-1}$, Studies in this region of $1200\text{-}1600\text{ cm}^{-1}$ becomes beneficial as some of the significant

IR bands of the Schiff base complexes like C=N, C=C, C-O stretching and C-H deformation emerging in this particular region, remain unaffected by host lattice.

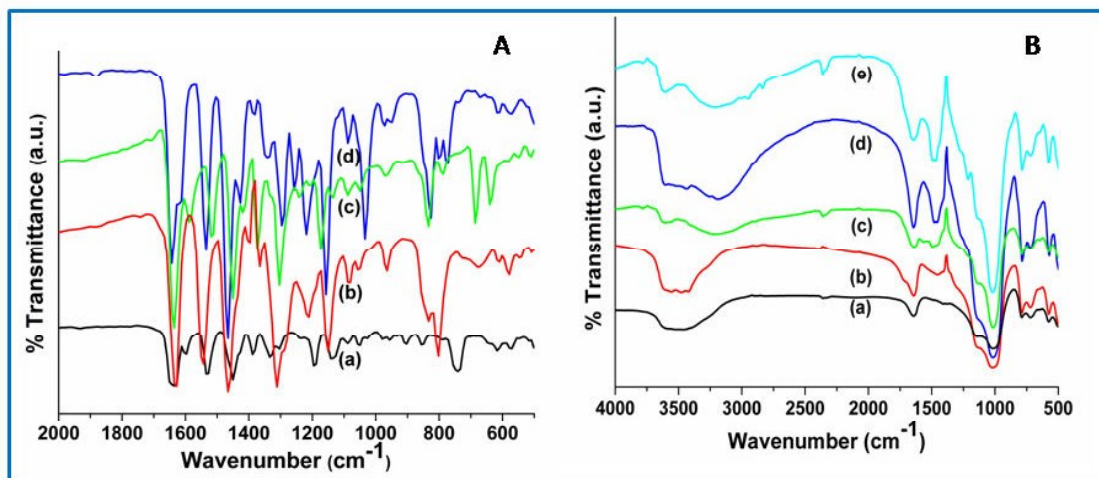


Figure 5.4: (A) FTIR spectra of free state copper salen complexes (a) CuL1, (b) CuL3, (c) CuL4 and (d) CuL6. (B) FTIR spectra of encapsulated copper salen complexes (a) pure zeolite Y, (b) CuL1-Y, (c) CuL3-Y, (d) CuL4-Y and (e) CuL6-Y.

Table 5.2: FTIR spectral data (in cm^{-1}) for neat and encapsulated state complexes.

S. No	Samples	C=N stretching	C=C stretching	$\nu_{\text{C-H}}$ deformation	C-O stretching
1	CuL1	1636	1535, 1450	1389	1304
2	CuL1-Y	1643	1450	1393	1303
3	CuL3	1628	1543, 1466	1389	1304
4	CuL3-Y	1643	1566, 1490	1396	1304
5	CuL4	1636	1520, 1450	1373	1304
6	CuL4-Y	1643	1458	1382	1304
7	CuL6	1643	1535, 1466	1389	1296
8	CuL6-Y	1643	1466	1394	1304

In the encapsulated complexes the C=N and C-O stretching bands are mainly shifted to lower wave numbers compared to that of the ligands and the higher shifts in $\nu_{\text{C-H}}$ deformation frequencies has already been attributed to the presence of complex inside the zeolite cavity²⁸. The observed FTIR spectral data (Table 5.2) suggest the formation of copper Schiff-base complexes in the free and encapsulated states inside the zeolite Y supercage.

5.2.4. X-Ray Photoelectron Spectroscopy (XPS)

The existence of the guest metal complex in zeolite Y is also confirmed with the help of XPS study, which is basically an indirect technique to investigate the location of metal complex in the host framework. The XPS survey spectra (Figures 5.5-5.7) and binding energy data of CuL1, CuL1-Y is presented in Table 5.3. It is observed that the elements/metal ions (C, N, O, Si, Al and Cu²⁺) are present in their respective surface chemical states in these complexes. The low concentration of metal contents in the encapsulated complexes makes the XPS signal for metal weak which is actually in accordance with the concentration dependent studies like IR, UV-Vis spectroscopy. The appearance of Cu (2p) peaks in XPS spectrum confirms the presence of copper and is assigned to the Cu 2p_{3/2} and Cu 2p_{1/2} confirms the +2 oxidation state of Cu and square planar geometry of the complexes in the free and encapsulated states. Cu 2p_{3/2} and Cu 2p_{1/2} XPS signals have appeared at the binding energies of 932.80 eV and 952.72 eV respectively for the CuL1 complex whereas for the encapsulated complexes (CuL1-Y) these peaks are slightly shifted towards the higher binding energies and have appeared at 934.13, 954.^{8,29}

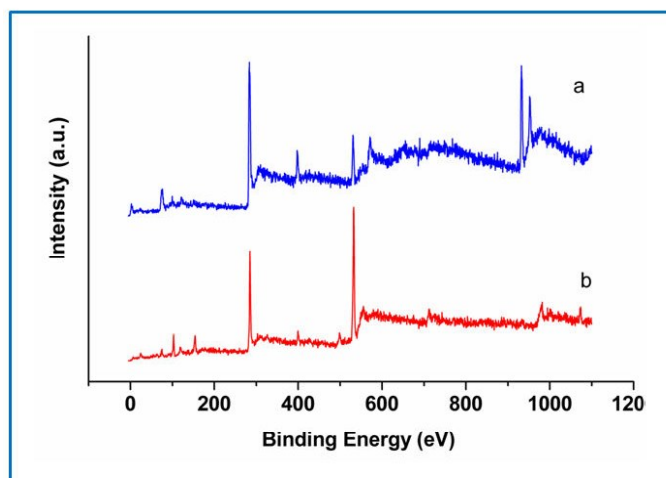


Figure 5.5: XPS survey spectra of (a) CuL1 and (b) CuL1-Y.

Such observed higher shifts in the binding energies upon encapsulation could be the result of lowering of electron density on the metal centre because of the impairment in the delocalization of electrons due to alteration in the square planar proximity of the encapsulated complexes.⁸ However, XPS signals for other atoms are more or less unshifted. C (1s) signals in the free state CuL1 complex appear at 283.35 and 285.03 eV, which corresponds to the sp²

and sp^3 carbon atoms, respectively.²⁹ N (1s) peaks for the complex are observed at binding energies 397.68 eV (M-N) and 399.61 eV (C=N) whereas O (1s) peaks appear at the binding energies of 531.26 eV (M-O) and 533.74 eV (C-O).²⁹ These XPS peaks are observed at almost identical binding energies for the encapsulated complex. For CuL1-Y complex, the C (1s) XPS signals are observed at 283.90, 285.76 eV and attributed to sp^2 , sp^3 carbon atom whereas signals at 397.65, 400.11eV and 530.80, 533.08 eV are attributed to (M-N, C=N) and (M-O, C-O) form of the respective elements, additionally the encapsulated complex has shown zeolitic Na (1s), Al (2p) and Si (2p) XPS signals at their respective positions. Comparative XPS binding energy data of both free and encapsulated complexes as well as higher shifts in binding energy for the Cu $2p_{3/2}$ and Cu $2p_{1/2}$ peaks in both encapsulated complexes essentially signify the encapsulation of metal complexes inside the zeolite Y.

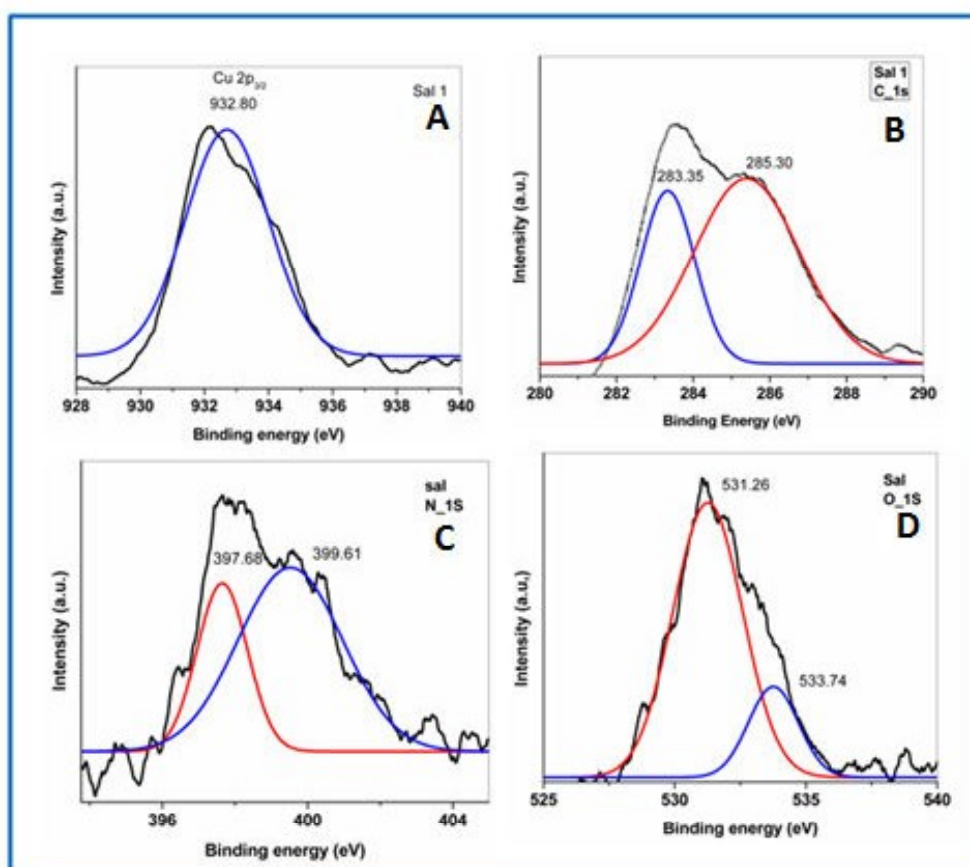


Figure 5.6: High resolution peak fitted XPS spectra of (A) Ni (2p) (B) C (1s), (C) N (1s) and (D) O (1s) for CuL1. (Black colored graphs are experimental data and red and blue colored peaks are peak fitted data)

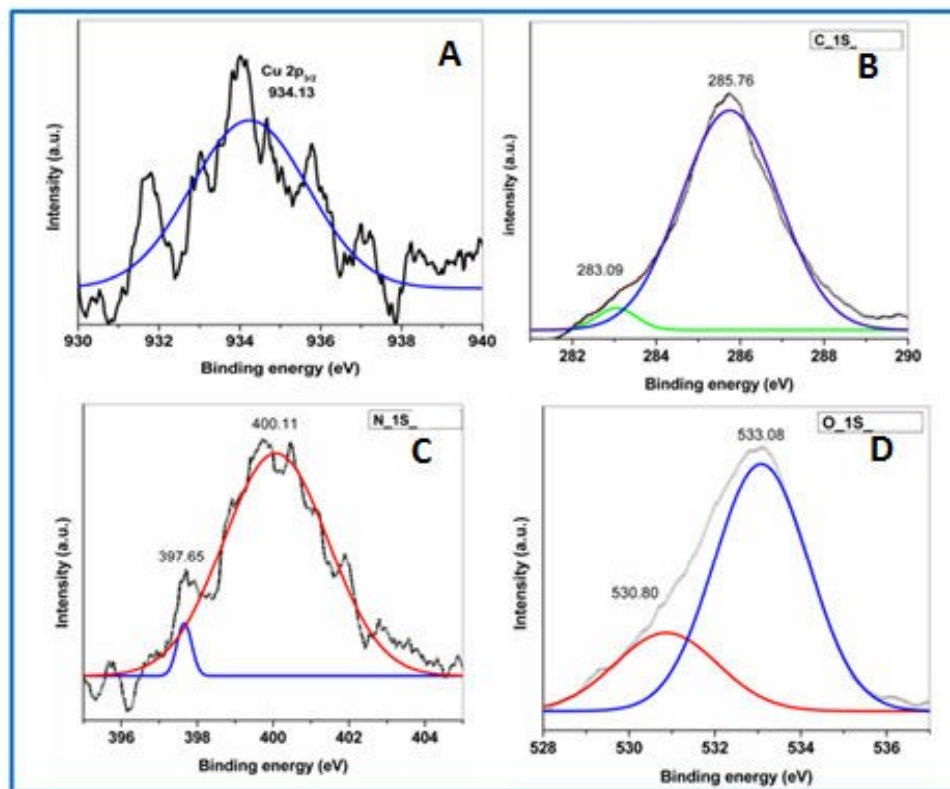


Figure 5.7: High resolution XPS spectra of (A) Ni (2p) (B) C (1s), (C) N (1s) and (D) O (1s) for CuL1-Y. (Black colored graphs are experimental data and red, green and blue colored peaks are peak fitted data)

Table 5.3 Binding energy (in eV) of the free and encapsulated complexes.

S. No	Samples	Si (2p)	Al (2p)	C (1s)	N (1s)	O (1s)	Cu ²⁺ (2p)
1	CuL1	-	-	283.35,	397.68,	531.26,	932.80,
				285.03	399.61	533.74	952.72
2	CuL1 -Y	103.46	75.21	283.90,	397.65,	530.80,	934.13,
				285.76	400.11	533.08	954.06

5.2.5. Solid state UV-Visible Study

To confirm the complex formation inside the cavity of zeolite and to study the co-ordination environment around the metal center, electronic spectroscopy is always being informative. The relative UV-Visible spectroscopic studies in solid state of all the copper Schiff-base complexes presented in Figure 5.8 and Table 5.4 thereby provide the significant evidences about the complex formation in the both states. Absorption bands in the range of (230-250) nm are recognized as $\pi-\pi^*$ transitions, where as in range of (300-384) nm are mainly assigned as $n-\pi^*$ transitions. The electronic transitions which are mainly originated from the metal d orbitals are identified in the comparative lower energy region of the spectrum. Bands appeared in the range of (404-471) nm and (502-607) nm are attributed to charge transfer and d-d transitions respectively. UV-Visible data of free CuL1 complex have shown good concurrence with the reported data in the literature³⁰ and also provided the information about the complex formation in the free state. After the encapsulation in zeolite Y, complexes have shown similar prototype of electronic spectra, indicating that the complexes are indeed present in the host lattice. Comparative studies of the electronic spectra of the complexes in free and their encapsulated states, make it quite clear that the intra-ligand transitions ($\pi-\pi^*$ and $n-\pi^*$) are relatively unaffected under the encapsulation; however transitions which are mainly instigated from the metal center are primarily altered in terms of peak positions as well as intensities for all considered guest complexes. It is quite interesting to perceive a regular blue shift and intensification of the d-d transitions in the encapsulated copper-Schiff base complexes. Such behavior already has been observed in the zeolite Y encapsulated complexes.²⁸ Observed modified electronic behavior in the d-d region is certainly an effect of different geometry of the co-ordination sphere, which the guest complex has adopted under the space restrictions of host supercage. Theoretical studies have also revealed the fact that changes in the bond angles, bond lengths and HOMO-LUMO gaps can be introduced in the guest complex by the process of encapsulation in zeolites.²⁷ In present study, the copper complexes have chosen on the basis of their molecular dimensions (i.e., end to end distances) of the complexes, which follow the order as CuL1 < CuL3 < CuL4 < CuL6 for the salen copper complexes. The complex with larger molecular dimensions experiences the more steric impulsion and obviously it adopts more distorted geometry to accommodate itself into the framework cavity. There are some interesting reports which have explored the

correlation between geometry of the metal complexes and different factors and their consequence. It is previously studied that effect of the substituent groups (-Cl and -OCH₃) on the geometry of copper Schiff-base complexes is so prominent.^{3, 31} Another report has revealed that the replacement of the atoms in the N₂O₂ square planar proximity by N₂OS and N₂S₂ leads the distortion in the geometry of that complex and its effect can be seen in the optical behavior of that complex.³²

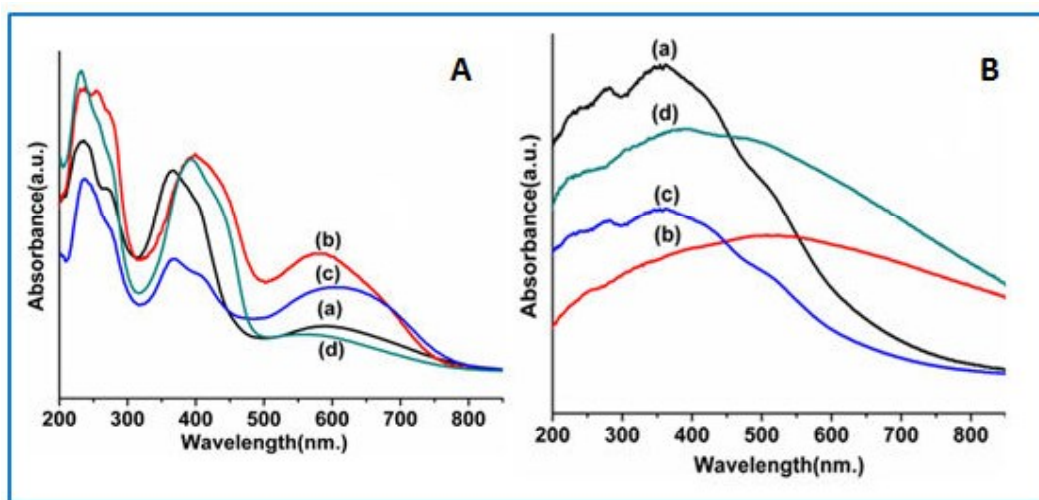


Figure 5.8: (A). Solid state UV-Vis spectra of free state copper salen complexes (a) CuL1, (b) CuL3, (c) CuL4 and (d) CuL6 (B). The solid state UV-Vis spectra of encapsulated copper salen complexes (a) CuL1-Y, (b) CuL3-Y, (c) CuL4-Y and (d) CuL6-Y.

Table 5.4: Solid state UV-Visible data (in nm) of copper Schiff-base complexes in free and encapsulated state.

S.No	Samples	$\pi-\pi^*$ transitions	$n-\pi^*$ transitions	CT transitions	d-d transitions
1	CuL1	232	364	404	592
2	CuL1-Y	234	362	417	533
3	CuL3	248	397	447	584
4	CuL3-Y	252	395	471	514
5	CuL 4	238	367	406	609
6	CuL4-Y	232	360	419	528
7	CuL6	232	391	435	592
8	CuL6-Y	241	387	418	495

A detailed study has suggested that the different substituent groups can cause the push-pull effect of on the porphyrin complexes which is really associated with the change in the energy gaps in the d-d orbitals.³³ In the present study we have observed a nice correlation in between the observed blue shift in d-d bands and the molecular dimensions of the copper Schiff base complexes. On encapsulation, the largest complex (CuL6) expected to adopt the most distorted geometry which is actually depicted as maximum blue shifted d-d bands in the electronic spectrum. The degree of blue shift in d-d bands is just in accordance to the increasing order of the molecular dimensions of complexes and the order is CuL1 < CuL3 < CuL4 < CuL6 for the salen complexes. This behavior of complexes is quite reasonable and can be correlated with the extent of distortion and molecular dimensions of the guest complex and their effects in their optical spectra.

5.2.6. Catalytic Study

To investigate catalytic activity of the encapsulated complexes, styrene oxidation transformation catalyzed by copper Schiff-base complexes in free and encapsulated state has been explored by using H₂O₂ as oxidant in the aerobic condition. Styrene can be oxidized into the different organic compounds like benzaldehyde, styreneoxide, benzoic acid, phenylacetaldehyde and phenylethane-1, 2-diol; some of these products of the reaction are previously reported.⁵ These products are identified and quantified with the help of Gas Chromatography by using internal standard method (calibration curve of styrene, benzaldehyde and styrene oxide are presented in Figure 5.9 A-C, GC chromatogram are given in Appendix A35-A42). Reaction conditions are optimized by considering the CuL1 complex in the encapsulated state as the representative catalyst and then by varying the different reaction parameters like temperature, time duration of reaction and amount of catalysts to attain maximum efficiency of these systems. In the various reaction conditions, styrene (1.56 g, 15 mmol) and 30% H₂O₂ (3.40 g, 30 mmol) are mixed with 15 ml acetonitrile and catalysts taken in different amounts (0.015g, 0.030g and 0.05g) at various temperatures 40°C, 80°C and 120°C for different reaction duration (2 hrs, 5 hrs and 8 hrs). Initially, the amount of catalysts is optimized for encapsulated CuL1 in zeolite Y as it has shown the improved reactivity, when employed in two different sets of reaction with 0.030g and 0.050g amounts. The conversion of styrene is found to the least when 0.015g amount catalyst is used (catalytic data are presented in Table 5.5-5.7). We have considered 0.050g as optimized

amount of the catalysts for above reaction conditions because there is not substantial improvement in the percentage conversion of styrene, when we have taken amount 0.070 g of the catalysts. The oxidation reaction of styrene (1.56 g, 15 mmol), 30% H₂O₂ (3.40 g, 30 mmol) with 15 ml acetonitrile and 0.050g catalyst has been kept for different time duration e.g., 2 hrs, 5 hrs and 8 hrs. The reactivity of catalysts is not much enhanced after 8 hrs and this is preferred as the adequate time for the above reaction to get the better efficiency. On above optimized conditions, the styrene oxidation reaction is studied at three different temperatures 40°C, 80°C and 120°C, and conversion of styrene quantified 4.66 %, 46.66 % and 58 % for encapsulated Sa11 complex at 40°C, 80°C and 120°C respectively. So 80°C temperature found the appropriate temperature for the reaction. Under these suitable conditions, copper salen complexes (CuL1, CuL3, CuL4 and CuL6) are employed as catalyst in free as well as encapsulated states (catalytic data are presented in Table 5.8). The amount of free state complexes has been taken in quite a low amount of 0.0045g in each case because of much higher concentration of metal centers in the complex compared to its analogous encapsulated state. These catalysts are more selective for benzaldehyde formation in both states while the other products like styrene oxide is a minor product and benzoic acid and phenylacetaldehyde are found in trace amounts. The conversion data are given in Table 5.8 The higher yield of benzaldehyde might be associated to the formation of hydroperoxystyrene intermediate by the nucleophilic attack of H₂O₂, which is further cleaved to produce benzaldehyde Another possibility of formation of benzaldehyde is further oxidation of styrene oxide which is one of the products of the styrene oxidation reaction (Scheme 5.1).³⁴ The formation of benzoic acid is the result of further oxidation of benzaldehyde and phenylacetaldehyde is the isomerized product of styrene oxide.³⁵

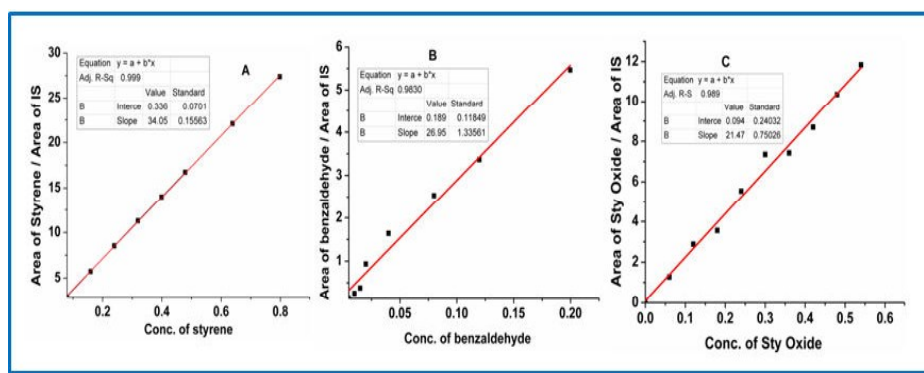


Figure 5.9: Calibration curves of (A) styrene, (B) benzaldehyde and (C) styrene oxide.

Table 5.5: Conversion of styrene using different amount of catalyst.

S.No	Amount of catalyst	% Conversion
1	0.015 g	16.66
2	0.03 g	23.33
3	0.05 g	46.66

Reaction conditions:- Styrene: 1.56 g, 15 mmol, H₂O₂: 3.40 g, 30 mmol, acetonitrile: 15 ml, temperature: 80⁰C and time duration: 8 hours.

Tables 5.6: Conversion of styrene using different temperature for the reaction.

S. No	Temp.	% Conversion
1	40 ⁰ C	4.66
2	80 ⁰ C	46.66
3	120 ⁰ C	58.00

Reaction conditions: Styrene:- 1.56 g, 15 mmol, H₂O₂: 3.40 g, 30 mmol, acetonitrile: 15 ml , time duration: 8 hours and catalyst: 0.05 g for encapsulated complex

Table 5.7: Conversion of styrene in different time durations.

S. No	Time	% Conversion
1	2 hrs	8.00
2	5 hrs	27.33
3	8 hrs	46.66

Reaction conditions:- Styrene: 1.56 g, 15 mmol), H₂O₂: 3.40 g, 30 mmol, acetonitrile 15 ml, temperature: 80⁰C, and catalyst: 0.05 g for encapsulated complex

Overall catalytic data have represented that the reactivity of free state copper Schiff-base follow the trend as CuL4> CuL1> CuL3 > CuL6 for salen complex. After encapsulation of complexes in the zeolite Y, there is certainly a significant reversal of the order. The catalytic reactivity order in the encapsulated state for the salen complexes is CuL6 > CuL4 > CuL1 > CuL3. The process of catalysis is definitely controlled by the electronic factor of the complexes when they are in free state however after encapsulation, steric factor imposed by the zeolite framework might have considerable contribution towards the catalytic activity.

Complexes with different substituent groups definitely offer different electronic environment for catalysis and additionally on encapsulation possibly they suffer from different steric hindrance which finally leads to the alteration of the activity order; the final structure of the encapsulated complex plays decisive role.

Table 5.8: Conversion of styrene after 8 hours reaction time with H₂O₂ as oxidant.

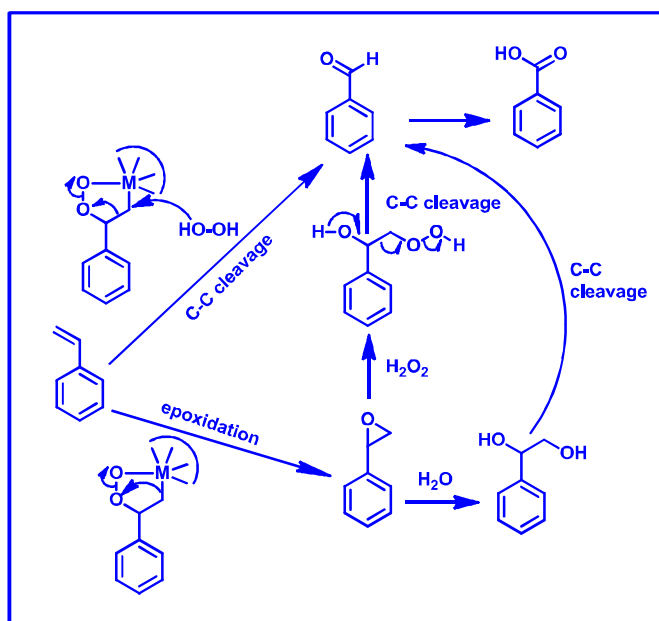
S. No	Samples	% Conversion	TON	Selectivity for Benz	Selectivity for SO
1	Zeolite-Y	3.10	-	-	-
2	CuL1	85.93	941.17	81.83	18.16
3	CuL1-Y	46.66	1435.31	96.35	3.79
4	CuL3	56	677.41	89.79	10.20
5	CuL3-Y	22.54	711.20	99.30	0.69
6	CuL4	76	1236.44	88.06	12.07
7	CuL4-Y	54.20	2793.81	91.64	8.35
8	CuL6	50.07	649.91	90.47	9.52
9	CuL6-Y	64.21	3137.25	96.28	4.24

Reaction conditions: (Styrene: 1.56 g, 15 mmol), (H₂O₂: 3.40 g, 30 mmol), acetonitrile 15 ml, temperature 80^oC, and catalyst (0.05 g for encapsulated complexes and 0.0045 g for neat complexes) **TON (turn over number):** mole of substrate converted per mole of metal center (encapsulated complexes).

5.2.7. Structural and functional Correlations

It is quite interesting to note that the reactivity in terms of turn over number (TON) of encapsulated complexes is significantly higher than the TON of free state complexes. That's why the zeolite encapsulated complexes have been attractive heterogeneous catalysts for various organic oxidative transformations.^{27, 35} The modified reactivity of the encapsulated complexes is mostly a consequence of the distorted geometry of the complexes, they adopt under encapsulation in zeolite Y. Copper Schiff-base complexes are generally efficient catalysts in solution as well as heterogeneous phases in comparisons to their corresponding nickel analogues. X-ray crystallographic study of these complexes evidently indicates that

copper metal is out of the square CuN_2O_2 proximity and shows distorted square planar geometry, where as nickel Schiff complex are slightly less distorted in comparison to the corresponding copper Schiff-base complex and retains its nearly square planar geometry.³⁶



Scheme 5.1: Purposed scheme for the oxidation of styrene.³⁴

When these complexes are encapsulated in zeolite Y, they are majorly distorted due to space constraint which is provided by rigid host zeolite supercage. Encapsulation causes distortion in geometry of the guest complex and as the result depletion in the electron density on the metal center happens. Comparative shifts towards higher value of binding energy in XPS signals for the zeolite encapsulated complexes also support the fact that encapsulation leads the generation of more electropositive metal center. It might be an exciting alternative approach for the formation of more electron deficient metal center with the help of induced structural distortion in guest complex by the rigid zeolite supercage.³ Lower the electron density on the metal center makes it more receptive for the nucleophilic attack. It has been also reported that when an electron withdrawing group (Cl) is attached to the copper salen complex the complex essentially becomes monomer in solid state and also has distorted square planar geometry around its planar proximity. The above report states that distorted chloro - copper salen complex provides the admixing of the ground state d_{xy} orbital with d_z^2 orbitals and thereby enhances the stability of electron-rich axial ligand complex.³¹ The same report has suggested that electron withdrawing group on the phenyl rings makes the metal

complex significantly away from planarity, however an electron donating group (-OCH₃) on the same position maintains the planarity of the complex. Planar conjugated systems make the metal center relatively higher electron density so that it acts as less efficient receptive center for the nucleophilic attacks. Recently, it is observed experimentally as well as theoretically that the nickel (II) Schiff-base complexes having different molecular dimensions adopt distorted geometry under encapsulation in zeolite Y. Largest complex experience more distortion and shows most enhanced catalytic activity for styrene oxidation after the encapsulation. Interestingly, this complex is least reactive for the same catalytic process in its free state (Discussed in chapter 3B and 3C). In the present study, parallel behavior of zeolite Y encapsulated copper salen complexes is observed for the oxidation of styrene in presence of H₂O₂. Detailed catalytic studies for the series of salen complexes have indicated that the CuL4 complex is the most reactive one among the lot for the styrene oxidation in free state. Electron withdrawing -Br group in CuL4 makes the complex distorted even in free state and as a consequence the complex is more reactive towards the nucleophilic attack and also can stabilize the electron-rich axial ligand (nucleophile) in the transition state. Encapsulation of CuL4 complex inside the supercage further enhances the degree of distortion and it could be an explanation of the higher reactivity of these systems. This behavior of the catalyst is well anticipated, because electronic factor of electron withdrawing groups and steric factors imposed by zeolite Y under encapsulation are the main decisive factors for activity of these systems which are additive and working in the same direction. CuL3 and CuL6 complexes are not as much reactive in their free states, which may be due to the existence of complexes in the dimeric form in their solution states,³¹ or generation of less receptive copper metal center for the nucleophilic attack of H₂O₂, since electron donating groups are attached on the phenyl rings. However these complexes when encapsulated in zeolite Y have shown very exciting catalytic behavior, CuL6 complex has shown remarkable enhanced reactivity for the above reaction. The competence of these heterogeneous systems is mainly driven by steric factor after encapsulation, which is in contrary to the electronic factor of substituent group (-OCH₃). The superior reactivity might be the outcome of the dominance of the steric factor over the electronic factor, since presence of two -OCH₃ groups on phenyl rings, make the complex comparatively larger and it is predictable that the complexes are more distorted to accommodate themselves inside the rigid host cavity of zeolite Y. It has been already established that the distortion makes the complex more reactive towards the oxidation

reaction by making the metal center more electropositive in nature. Encapsulated CuL3 complex having electron donating substituent and with moderate molecular dimensions are not effective for catalytic oxidation of styrene molecule as CuL6 complex in their encapsulated states. For CuL3 complex, electronic and steric effects oppose each other and are almost comparable to each other, so efficiency of these systems remains moderate even after encapsulation in the zeolite Y.

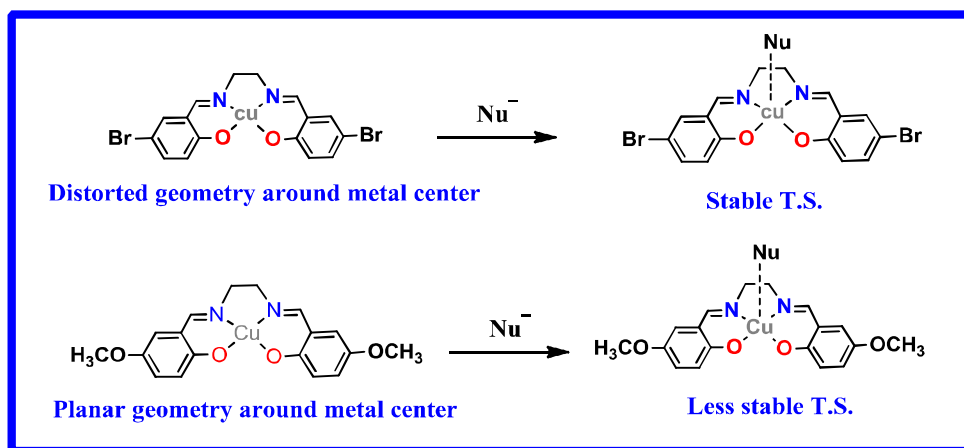


Figure 5.10: Effect of substituent's on the geometry of complex around the metal and its effect on the transition state (T.S.) during the nucleophilic attack.

Overall catalytic data have represented that the reactivity of free state copper Schiff-base complexes are mainly driven by the electronic factors and the trend for catalytic reactivity of the complexes follow the order of $\text{CuL4} > \text{CuL1} > \text{CuL3} > \text{CuL6}$ for salen complexes. After encapsulation of complexes in the zeolite Y, the reactivity order is mainly determined by molecular dimensions and extent of distortion of the guest complexes. The catalytic reactivity order in the encapsulated state for the salen complexes therefore becomes $\text{CuL6} > \text{CuL4} > \text{CuL1} > \text{CuL3}$. Experimentally observed blue shift in d-d in electronic data also support above catalytic order of the encapsulated complexes.

5.3. CONCLUSION

Zeolite framework certainly provides a choice to design the heterogeneous catalyst with customized reactivity by the encapsulation process. Rigid walls of framework impose space restraint on the guest complex forcing the guest complex to adopt distorted structure. Such alteration in the structure of the complex plays a crucial role for the modified reactivity of the

system. Blue shifted d-d bands in electronic spectra signify the alternation in the metal d orbitals energy levels, which is surely an effect of the altered coordination sphere of the metal center. This adaptation finally leads towards the non-planar geometry and as a result the formation of more electropositive metal center due to impediment in the conjugation of the system takes place. The shift towards higher binding energy in Cu_{2p3} (II) XPS signal for the encapsulated complexes apparently indicates the generation of more susceptible electropositive metal center for the nucleophilic attack of H₂O₂. It is obvious that the larger molecular dimension leads more deformation in geometry of complex and as an effect the creation of more catalytically-active metal center in the encapsulated state of the complex.

REFERENCES

1. A. R. Dick, K. L. Hull and M. S. Sanford, *J. Am. Chem. Soc.*, 2004, **126**, 2300-2301.
2. N. Y. Chen and W. E. Garwood, *J. Catal.*, 1978, **52**, 453-458.
3. S. Deshpande, D. Srinivas and P. Ratnasamy, *J. Catal.*, 1999, **188**, 261-269.
4. J. R. Anderson, K. Foger, T. Mole, R. A. Rajadhyaksha and J. V. Sanders, *J. Catal.*, 1979, **58**, 114-130.
5. M. R. Maurya, A. K. Chandrakar and S. Chand, *J. Mol. Catal. A: Chem.*, 2007, **274**, 192-201.
6. C. Jin, W. Fan, Y. Jia, B. Fan, J. Ma and R. Li, *J. Mol. Catal. A: Chem.*, 2006, **249**, 23-30.
7. K. J. Balkus and A. G. Gabrielov, in *Inclusion Chemistry with Zeolites: Nanoscale Materials by Design*, eds. N. Herron and D. R. Corbin, Springer Netherlands, Dordrecht, 1995, DOI: 10.1007/978-94-011-0119-6_6, pp. 159-184.
8. K. K. Bania and R. C. Deka, *J. Phys. Chem. C*, 2013, **117**, 11663-11678.
9. J. Zhu, Z. Kónya, V. F. Puentes, I. Kiricsi, C. X. Miao, J. W. Ager, A. P. Alivisatos and G. A. Somorjai, *Langmuir*, 2003, **19**, 4396-4401.
10. D. E. De Vos, M. Dams, B. F. Sels and P. A. Jacobs, *Chem. Rev.*, 2002, **102**, 3615-3640.
11. C.-Y. Sun, X.-L. Wang, X. Zhang, C. Qin, P. Li, Z.-M. Su, D.-X. Zhu, G.-G. Shan, K.-Z. Shao, H. Wu and J. Li, *Nature Communications*, 2013, **4**, 2717.
12. P. Ling, J. Lei, L. Zhang and H. Ju, *Anal. Chem.*, 2015, **87**, 3957-3963.
13. Q. Yao and Y. Zhang, *Angew. Chem. Int. Ed. (English)*, 2003, **42**, 3395-3398.

14. I. J. B. Lin and C. S. Vasam, *J. Organomet. Chem.*, 2005, **690**, 3498-3512.
15. M. Cinouini, S. Colonna, H. Molinari, F. Montanari and P. Tundo, *J. Chem. Soc., Chem. Commun.*, 1976, DOI: 10.1039/C39760000394, 394-396.
16. X. Zuwei, Z. Ning, S. Yu and L. Kunlan, *Science*, 2001, **292**, 1139-1141.
17. F. Bedioui, *Coord. Chem. Rev.*, 1995, **144**, 39-68.
18. R. F. Parton, I. F. J. Vankelecom, M. J. A. Casselman, C. P. Bezoukhanova, J. B. Uytterhoeven and P. A. Jacobs, *Nature*, 1994, **370**, 541-544.
19. M. R. Maurya, A. K. Chandrakar and S. Chand, *J. Mol. Catal. A: Chem.*, 2007, **263**, 227-237.
20. M. R. Maurya, A. K. Chandrakar and S. Chand, *J. Mol. Catal. A: Chem.*, 2007, **270**, 225-235.
21. B. Neelam, N. Fehmida, B. Alok, B. Sudha and A. Amir, *European journal of medicinal chemistry*, 2000, **35**, 481-486.
22. M. Maurya, S. Titinchi, S. Chand and I. Mishra, *J. Mol. Catal. A: Chem.*, 2002, **180**, 201-209.
23. M. R. Maurya, S. J. Titinchi and S. Chand, *J. Mol. Catal. A: Chem.*, 2003, **201**, 119-130.
24. M. Martis, K. Mori and H. Yamashita, *Dalton Trans.*, 2014, **43**, 1132-1138.
25. S. Seelan and A. K. Sinha, *Appl. Catal., A*, 2003, **238**, 201-209.
26. W. H. Quayle, G. Peeters, G. L. De Roy, E. F. Vansant and J. H. Lunsford, *Inorg. Chem.*, 1982, **21**, 2226-2231.
27. K. K. Bania, D. Bharali, B. Viswanathan and R. C. Deka, *Inorg. Chem.*, 2012, **51**, 1657-1674.
28. R. Ganesan and B. Viswanathan, *J. Phys. Chem. B*, 2004, **108**, 7102-7114.
29. G. Ramanjaneya Reddy, S. Balasubramanian and K. Chennakesavulu, *J. Mater. Chem. A*, 2014, **2**, 15598-15610.
30. S. Koner, *Chem. Commun.*, 1998, DOI: 10.1039/A707681I, 593-594.
31. M. M. Bhadbhade and D. Srinivas, *Inorganic Chemistry*, 1993, **32**, 6122-6130.
32. L. Gomes, E. Pereira and B. de Castro, *Journal of the Chemical Society, Dalton Transactions*, 2000, DOI: 10.1039/A908330H, 1373-1379.
33. N. Grover, M. Sankar, Y. Song and K. M. Kadish, *Inorganic Chemistry*, 2016, **55**, 584-597.

34. T. A. G. Duarte, A. C. Estrada, M. M. Q. Simoes, I. C. M. S. Santos, A. M. V. Cavaleiro, M. G. P. M. S. Neves and J. A. S. Cavaleiro, *Catal. Sci. Technol.*, 2015, **5**, 351-363.
35. M. R. Maurya, B. Singh, P. Adão, F. Avecilla and J. Costa Pessoa, *European Journal of Inorganic Chemistry*, 2007, **2007**, 5720-5734.
36. A. Boettcher, H. Elias, E. G. Jaeger, H. Langfelderova, M. Mazur, L. Mueller, H. Paulus, P. Pelikan, M. Rudolph and M. Valko, *Inorganic Chemistry*, 1993, **32**, 4131-4138.



This document was created with the Win2PDF "print to PDF" printer available at <http://www.win2pdf.com>

This version of Win2PDF 10 is for evaluation and non-commercial use only.

This page will not be added after purchasing Win2PDF.

<http://www.win2pdf.com/purchase/>